



1 **Soil water content and salinity regulate the temperature sensitivity of**

2 **CO<sub>2</sub> and CH<sub>4</sub> emissions in a coastal salt-affected land**

3 Mengmeng Diao<sup>a,b,1</sup>, Wenyao Sun<sup>a,1</sup>, Zhaosong Zhang<sup>a,1</sup>, Yitong Chen<sup>c</sup>, Qian Zhang<sup>a</sup>,

4 Xiang Ma<sup>a</sup>, Juan Sun<sup>a,b</sup>, Chao Yang<sup>a,b\*</sup>

5 <sup>a</sup> College of Grassland Science, Qingdao Agricultural University, Qingdao, China

6 <sup>b</sup> Shandong Key Laboratory for Germplasm Innovation of Saline-alkaline Tolerant

7 Grasses and Trees, Qingdao, China

8 <sup>c</sup> College of Grassland Agriculture, Northwest A&F University, Yangling, China

9 <sup>1</sup> These authors contributed equally

10 \* Corresponding Author: yangchao@qau.edu.cn



11 **Abstract**

12 Soil carbon emissions from coastal saline-alkaline ecosystems significantly influence the  
13 global carbon cycle, yet their responses to key environmental drivers such as soil water content  
14 and salinity remain insufficiently understood. This study employed controlled incubation  
15 experiments using soils collected from the Yellow River Delta, China, to systematically  
16 investigate the effects of varying soil water content (5%, 15%, 30%, 45%, and 60%) and salinity  
17 levels (S1: EC=1.9 dS/m; S2: 10.8 dS/m; S3: 58.8 dS/m; S4: 66.3 dS/m; S5: 96.0 dS/m) on CO<sub>2</sub>  
18 and CH<sub>4</sub> emissions and their temperature sensitivity (Q<sub>10</sub>). The results demonstrated that under  
19 constant temperature conditions, CO<sub>2</sub> emission flux followed a unimodal pattern in response to  
20 increasing soil water content, peaking at 45% water content, with CH<sub>4</sub> flux exhibiting a similar  
21 trend. Soil salinity significantly suppressed the fluxes of both greenhouse gases, with reductions  
22 observed across all temperature levels as salinity increased. Both soil water content and salinity  
23 played substantial regulatory roles in modulating the Q<sub>10</sub> of gas emissions. Specifically, Q<sub>10</sub>  
24 values for CO<sub>2</sub> and CH<sub>4</sub> initially decreased and then increased with rising soil water content.  
25 Along the salinity gradient, the Q<sub>10</sub> of CO<sub>2</sub> decreased from S2 to S4, whereas the Q<sub>10</sub> of CH<sub>4</sub>  
26 increased progressively from S2 to S5. These findings reveal the complex and interactive effects  
27 of soil water content and salinity on carbon cycling processes in coastal saline-alkaline lands.  
28 The study provides crucial theoretical insights for improving the prediction of carbon cycle  
29 dynamics under climate change and offers a scientific basis for the adaptive management and  
30 conservation of these vulnerable ecosystems.

31 **Keywords:** Coastal saline-alkaline land; Soil water content; Soil salinity; CO<sub>2</sub> and CH<sub>4</sub>  
32 emissions; Temperature sensitivity (Q<sub>10</sub>)



## 33 1. Introduction

34 Saline-alkaline lands are strategically significant for enhancing regional carbon sinks and mitigating  
35 global environmental change (Ma et al. 2024). Their unique stressors (e.g., high salinity and osmotic pressure)  
36 alter soil properties and biogeochemical cycles, regulating organic carbon preservation and carbon pool  
37 stability (Wong et al. 2010). While greenhouse gas research has largely focused on non-saline soils—  
38 typically CO<sub>2</sub> sources and CH<sub>4</sub> sinks, with positive CH<sub>4</sub> fluxes mainly in wetlands (Gao et al. 2018, Zhan et  
39 al. 2023)—drivers of gas fluxes in saline-alkaline soils remain poorly understood (Tang et al. 2016, Feng et  
40 al. 2022). Existing studies concentrate on inland saline lands (Wang et al. 2021), leaving coastal systems,  
41 with distinct salinity and hydrological dynamics, understudied. Investigating carbon emissions in coastal  
42 saline-alkaline lands is thus critical, especially as soil salinization constrains emission reduction efforts in  
43 China (Huang et al. 2024).

44 The temperature sensitivity ( $Q_{10}$ ) of greenhouse gas emissions—the increase per 10 °C rise—is a key  
45 parameter in climate-carbon feedback models (Alster et al. 2018).  $Q_{10}$  of soil respiration varies with  
46 temperature, soil water content, soil properties, microbial communities, and vegetation (Lloyd et al. 1994,  
47 Wang et al. 2014), generally higher in cold ecosystems due to microbial reliance on recalcitrant carbon (Li  
48 et al. 2020, Li et al. 2021). For example, temperate forests show higher  $Q_{10}$  than tropical forests, linked to  
49 microbial composition and carbon quality (Johnston et al. 2018, Wang et al. 2018). However,  $Q_{10}$  studies in  
50 saline-alkaline lands are scarce, limiting understanding under global warming.

51 Soil water content regulates carbon gas production and emissions by affecting redox potential, aeration,  
52 microbial activity, and diffusion (Capooci et al. 2019). Optimal soil water content supports microbial  
53 activity, while extremes suppress it (Cao et al. 2023). Soil water content effects on respiration vary spatially  
54 and temporally (Schaufler et al. 2010, Wang et al. 2013, Gao et al. 2018), and drive CH<sub>4</sub> flux thresholds—  
55 uptake at 30–60% field capacity, emission at 75–90% (Suh et al. 2009). Soil water content also interacts  
56 with temperature to indirectly influence  $Q_{10}$  (Hansen et al. 2013).

57 Salinity critically regulates carbon cycles in coastal wetlands (Ho et al. 2024). It reduces CO<sub>2</sub> production  
58 potential by decreasing labile carbon and inhibiting microbial metabolism (Huang et al. 2019), while  
59 suppressing CH<sub>4</sub> oxidation (Saari et al. 2004). Low salinity can enhance CH<sub>4</sub> uptake, whereas high salinity  
60 induces osmotic stress and toxicity, inhibiting microbial activity and diversity (Pathak et al. 1998). Warming



61 further stimulates CO<sub>2</sub> emissions by accelerating organic matter decomposition (SUN et al. 2016).

62 China has extensive saline-alkaline land  $9.9 \times 10^6$  ha (Liu et al. 2024). The Yellow River Delta, a  
63 dynamic coastal delta with severe salinization (50.9% saline soil)(Ma et al. 2025), is ideal for studying these  
64 interactions. This study examines how soil water content and salinity affect CO<sub>2</sub> and CH<sub>4</sub> emissions and their  
65 temperature sensitivity through incubation experiments, providing insights into the role of saline-alkaline  
66 lands in the carbon cycle and their response to climate change. This study proposes the following three core  
67 hypotheses: 1) soil water content will significantly regulate CO<sub>2</sub> and CH<sub>4</sub> emission fluxes and their  
68 temperature sensitivity ( $Q_{10}$ ) in saline-alkaline soil. An optimal soil water content threshold is expected,  
69 beyond or below which emissions are suppressed, and increased soil water content may decrease the  $Q_{10}$  of  
70 CO<sub>2</sub> emissions. 2) Elevated salinity will inhibit the emission potential of CO<sub>2</sub> and CH<sub>4</sub> and alter their  $Q_{10}$ .  
71 Salinity directly weakens emission intensity by suppressing microbial and enzymatic activities, and may  
72 indirectly affect  $Q_{10}$  by altering substrate availability. 3) There will be significant interactive effects between  
73 soil water content and salinity on greenhouse gas emissions and their  $Q_{10}$ . Under high temperatures, high  
74 salinity may exacerbate the suppression of microbial activity due to water stress, thereby significantly  
75 reducing the  $Q_{10}$  of CO<sub>2</sub> emissions. For CH<sub>4</sub>, the interaction between soil water content and salinity is likely  
76 to dominate the balance between production and oxidation processes, ultimately determining the net  
77 emission direction and the strength of the temperature response.

## 78 **2. Materials and methods**

### 79 **2.1. Study Site**

80 Soil samples were collected from a coastal saline-alkaline area within the Agricultural High-tech  
81 Industrial Demonstration Zone of the Yellow River Delta, Dongying City, Shandong Province, China  
82 (37.3°N, 118.7°E; ~6.7 m altitude) (Yang et al. 2025). The region has a warm temperate monsoon climate  
83 characterized by distinct seasonal variation, with a mean annual temperature of 12.8°C and mean annual  
84 precipitation of 555.9 mm, predominantly in summer. The soil is classified as coastal saline-alkaline,  
85 covering approximately 36% of Dongying City's total soil area along the Bohai Sea coast.

### 86 **2.2. Soil Sampling and Analysis**

87 In May 2022, soil sampling was conducted across the main salinity gradients of the study area.  
88 Based on vegetation distribution, ten 50-meter transects were randomly established. Five sampling



89 points were randomly selected along each transect, resulting in 50 points in total (Yang et al. 2025).

90 Topsoil (0–20 cm depth) was collected at each point using a soil corer. Soils from points with identical  
91 vegetation types were composited, placed in sealed polyethylene bags, and transported to the laboratory.

92 The composited samples were air-dried, passed through a 2-mm sieve to remove roots and debris,  
93 and homogenized. A subsample was then analyzed for key physicochemical properties: electrical  
94 conductivity (EC, measured in a 1:5 soil:water extract), pH (determined in a 1:5 soil:water suspension),  
95 and total carbon (TC) and total nitrogen (TN) via elemental analysis. Based on EC values, soils were  
96 categorized into five salinity gradients (S1–S5), representing a spectrum from non-saline to extremely  
97 saline conditions (Table 1). The remaining soil was stored for incubation experiments.

### 98 **2.3. Incubation Experiment Design**

99 Air-dried soil was packed into PVC columns (20 cm diameter × 30 cm height), with a 10-cm  
100 headspace for gas sampling and a sealed bottom (Fig. S1). To isolate the effects of salinity and soil  
101 water content, two controlled incubation experiments were conducted across a temperature gradient (5,  
102 10, 15, 20, 25, and 30°C): 1) Salinity experiment: Five salinity levels (S1–S5) were incubated at  
103 constant soil water content (60% water content). 2) Soil water content experiment: Five soil water  
104 content levels (5%, 15%, 30%, 45%, 60%) were incubated using soil from the lowest salinity gradient  
105 (S1). Each treatment combination had five replicates, totaling 150 experimental units. soil water content  
106 was maintained by weighing and replenishing with deionized water every 1–2 days. Temperature was  
107 controlled using artificial climate chambers. After a 7-day stabilization period at each target temperature,  
108 gas fluxes were measured.

### 109 **2.4. Gas Flux Measurement**

110 CO<sub>2</sub> and CH<sub>4</sub> fluxes were measured using a portable greenhouse gas analyzer (LI-7810, LI-COR  
111 Biosciences, USA). Measurements were taken between 9:00 and 11:00 local time. For each column,  
112 three consecutive flux readings were recorded and averaged. Flux measurements were conducted over  
113 a 10-day period at each temperature. The instrument was calibrated before each session (calibration  
114 error ≤ 1%).

### 115 **2.5. Statistical Analysis**

116 Data were processed and analyzed using Microsoft Excel 2019 and SPSS 19.0. The effects of



117 experimental factors (salinity, soil water content, temperature, and their interactions) were tested using  
118 one-way and two-way analysis of variance (ANOVA). Where ANOVA indicated significant effects ( $P$   
119  $< 0.05$ ), post-hoc comparisons among treatment groups were performed using the Least Significant  
120 Difference (LSD) test. All results are reported as the mean  $\pm$  standard error (SE).

121 The relationship between soil respiration rate ( $R$ ) and incubation temperature ( $T$ ) was modeled  
122 using an exponential function:  $R = ae^{(bT)}$

123 where  $a$  is the theoretical respiration rate at  $0^\circ\text{C}$  and  $b$  is the temperature sensitivity coefficient.

124 The temperature sensitivity index,  $Q_{10}$  (representing the factor change in respiration rate per  $10^\circ\text{C}$   
125 increase in temperature), was calculated as:  $Q_{10} = e^{(10b)}$

126 The parameter  $b$  was estimated for each salinity or soil water content gradient via nonlinear  
127 regression, and the corresponding  $Q_{10}$  values were derived and reported as mean  $\pm$  SE (Lang et al. 2017).

128 Data visualization and figure generation were completed using Origin 2020.

### 129 **3. Results**

#### 130 **3.1. Effects of soil water content on $\text{CO}_2$ and $\text{CH}_4$ emissions and their temperature sensitivity**

131 Soil  $\text{CO}_2$  emission flux demonstrated a strong positive correlation with temperature across the  
132 entire soil water content gradient (5%, 15%, 30%, 45%, and 60%). At each fixed soil water content  
133 level, flux increased significantly ( $P < 0.05$ ) with rising incubation temperature from  $5^\circ\text{C}$  to  $30^\circ\text{C}$ .  
134 Conversely, under a constant temperature,  $\text{CO}_2$  flux exhibited a distinct unimodal relationship with soil  
135 water content: it initially increased, peaked at 45% soil water content, and subsequently decreased.  
136 Differences in  $\text{CO}_2$  flux among soil water content treatments at the same temperature were statistically  
137 significant ( $P < 0.05$ ). The highest mean  $\text{CO}_2$  flux was observed under the combined condition of  $30^\circ\text{C}$   
138 and 45% soil water content, whereas the lowest flux occurred at  $5^\circ\text{C}$  and 60% soil water content (Fig.  
139 1). The temperature sensitivity ( $Q_{10}$ ) of  $\text{CO}_2$  emissions varied between 1.48 and 1.87 across soil water  
140 content treatments. Interestingly,  $Q_{10}$  itself showed a unimodal response to increasing water content,  
141 reaching its minimum value of 1.48 at 45% soil water content (Table 2).

142 Soil acted as a net source of  $\text{CH}_4$  across all experimental conditions, with emission fluxes  
143 consistently positive.  $\text{CH}_4$  flux displayed a similar response pattern to  $\text{CO}_2$ : a significant increase with  
144 temperature ( $P < 0.05$ ) under constant soil water content, and a unimodal relationship with soil water



145 content under constant temperature, again maximizing at 45% soil water content. Fluxes differed  
146 significantly ( $P < 0.05$ ) among soil water content levels at a given temperature. Peak  $\text{CH}_4$  emission was  
147 recorded at 30°C and 45% soil water content, while the minimum was found at 5°C and 5% soil water  
148 content (Fig. 2). The  $Q_{10}$  for  $\text{CH}_4$  emissions ranged from 1.13 to 1.29, mirroring the trend observed for  
149  $\text{CO}_2$  by declining to its lowest value (1.13) at the optimal soil water content content of 45% (Table 2).

150 These patterns were further validated by exponential models fitted to the data (Fig. 3 and 4). The  
151 models confirmed that for both gases, flux at constant temperature first rose and then fell with increasing  
152 soil water content, while at constant soil water content, flux increased exponentially with temperature.  
153 A highly significant positive correlation ( $P < 0.01$ ) was found between the treatment variables  
154 (temperature  $\times$  soil water content) and gas fluxes. Regression analysis indicated that soil temperature  
155 alone explained 34.7–58.2% of the variance in  $\text{CO}_2$  flux, and 3–10% of the variance in  $\text{CH}_4$  flux across  
156 treatments ( Figs. 2 and 3).

### 157 **3.2. Effects of Soil Salinity on $\text{CO}_2$ and $\text{CH}_4$ Emissions and their temperature sensitivity**

158 All soils, regardless of salinity gradient (S1 to S5, with S1 being lowest), functioned as net sources  
159 of  $\text{CO}_2$  under the experimental conditions (Fig. 5). However, the nature of the temperature response was  
160 modulated by salinity level. For gradients S1, S2, and S5,  $\text{CO}_2$  flux generally increased with rising  
161 temperature, though significant differences ( $P < 0.05$ ) were not always present between adjacent  
162 temperature points (e.g., between 20°C and 25°C in S2). In contrast, the S3 gradient exhibited an  
163 atypical response, with peak flux occurring at 20°C, which was significantly higher ( $P < 0.05$ ) only than  
164 fluxes at 5°C, 10°C, and 15°C. The S4 gradient showed a bell-shaped response, with flux increasing up  
165 to 25°C before declining at 30°C. The  $Q_{10}$  for  $\text{CO}_2$  emissions across salinity levels ranged from 1.44 to  
166 1.75 (Table 3).

167 A clear inhibitory effect of salinity on  $\text{CO}_2$  flux was observed. Across all incubation temperatures,  
168 mean flux significantly decreased with increasing salinity gradient. The specific pattern of significant  
169 differences among gradients was temperature-dependent. At lower temperatures (e.g., 10°C, 15°C), the  
170 low-salinity gradients (S1, S2) often showed significantly higher fluxes ( $P < 0.05$ ) than the higher-  
171 salinity ones (S3-S5). At higher temperatures (e.g., 20°C, 25°C), the lowest salinity gradient (S1) was  
172 typically significantly different ( $P < 0.05$ ) from all others, while differences among higher-salinity



173 gradients were less consistent.

174 Salinity exerted a significant influence on CH<sub>4</sub> emissions (Fig. 6). Similar to CO<sub>2</sub>, CH<sub>4</sub> flux  
175 increased with temperature for all salinity levels ( $P < 0.05$ ). However, at a fixed temperature, CH<sub>4</sub> flux  
176 displayed a general decreasing trend with increasing salinity. This suppression by high salinity was  
177 statistically significant ( $P < 0.05$ ) at lower incubation temperatures (5°C, 10°C, 15°C). Notably, at  
178 higher temperatures ( $\geq 20^\circ\text{C}$ ), although the decreasing trend persisted, differences in CH<sub>4</sub> flux among  
179 the various salinity gradients were no longer statistically significant ( $P > 0.05$ ). The temperature  
180 sensitivity of CH<sub>4</sub> emissions ( $Q_{10}$ ) increased with salinity, ranging from 1.12 at the lowest salinity to  
181 1.39 at the highest (Table 3).

182 Exponential modeling revealed a consistent and significant negative correlation ( $P < 0.05$ ) between  
183 both CO<sub>2</sub> and CH<sub>4</sub> emission fluxes and soil salinity at each individual temperature level (Fig. 7 and 8).  
184 Conversely, under a constant salinity level, a significant positive correlation ( $P < 0.05$ ) was observed  
185 between gas fluxes and incubation temperature (Figs. 4 and 5).

#### 186 **4. Discussion**

187 This study elucidates the individual and interactive regulatory roles of soil water content and  
188 salinity on CO<sub>2</sub> and CH<sub>4</sub> emissions and their temperature sensitivity ( $Q_{10}$ ) in a coastal saline-alkaline  
189 ecosystem. Our results robustly support the proposed hypotheses. First, soil water content exhibited a  
190 pronounced unimodal effect on the fluxes of both gases, with an optimal threshold around 45%, aligning  
191 with Hypothesis 1. Notably, the  $Q_{10}$  values for both CO<sub>2</sub> and CH<sub>4</sub> were also minimized at this soil water  
192 content level, confirming soil water content's critical role in modulating temperature response. Second,  
193 increasing salinity significantly suppressed the emission potential of CO<sub>2</sub> and CH<sub>4</sub> across most  
194 temperatures, consistent with Hypothesis 2. Furthermore, salinity altered the  $Q_{10}$ , particularly for CH<sub>4</sub>  
195 emissions where sensitivity increased with salinity. Finally, significant interactive effects were observed  
196 (Hypothesis 3). The suppressive effect of high salinity on emissions was often most pronounced at lower  
197 temperatures, and the inhibitory effect of salinity on CH<sub>4</sub> flux became less distinct at higher  
198 temperatures ( $\geq 20^\circ\text{C}$ ), indicating a complex temperature-soil water content-salinity interplay  
199 governing microbial processes.

#### 200 **4.1. The unimodal moisture response and its impact on $Q_{10}$**



201           The unimodal relationship between gas flux and soil water content is a classic pattern, typically  
202 attributed to opposing constraints (Peng et al. 2025). This study, along with previous work, demonstrates  
203 that CO<sub>2</sub> and CH<sub>4</sub> emission fluxes exhibit this classic unimodal relationship with soil water content,  
204 with the optimal threshold generally occurring in the medium soil water content range (e.g., around  
205 45%). This pattern results from the physical constraints of soil water content on microbial activity and  
206 substrate diffusion, as well as its regulation of redox conditions (Yin et al. 2025). Under low soil water  
207 content conditions (e.g., 5%–15%), water deficit directly limits microbial physiological activity and the  
208 diffusion of substrates such as soluble organic carbon, thereby inhibiting gas emissions. Under these  
209 conditions, soils often act as a net sink for CH<sub>4</sub> because aerobic methanotroph activity dominates (Wang  
210 et al. 2025).

211           When soil water content increases to the optimal level, these physical constraints are alleviated.  
212 For CO<sub>2</sub> emissions, suitable water content optimizes soil aeration, significantly promoting microbial  
213 metabolic activity dominated by aerobic respiration, which drives CO<sub>2</sub> release to its peak (Ma et al. 2024,  
214 Niu et al. 2024). For CH<sub>4</sub> emissions, this soil water content range creates a delicate balance: on one hand,  
215 it provides favorable anaerobic microsites for methanogens, promoting CH<sub>4</sub> production; on the other  
216 hand, the soil maintains a certain capacity for oxygen diffusion, allowing aerobic methane oxidation to  
217 partially proceed. This dynamic balance between methanogenesis and methane oxidation leads to the  
218 peak net CH<sub>4</sub> flux (Gondwe et al. 2021). Water content conditions, by influencing the accumulation and  
219 spatial distribution of soluble organic carbon, profoundly affect microbial activity and function, thereby  
220 serving as a key mechanism driving changes in emission fluxes (Yang et al. 2022). When water content  
221 exceeds the optimal threshold (e.g., >50%), soil pores approach water saturation, severely impeding  
222 oxygen diffusion. This shift redirects the dominant microbial metabolic pathway from efficient aerobic  
223 respiration to less efficient anaerobic fermentation pathways, thereby suppressing CO<sub>2</sub> production  
224 (Zeeshan et al. 2022). For CH<sub>4</sub>, while strongly anaerobic conditions favor methanogenesis, excessively  
225 high soil water content may simultaneously inhibit methanotroph activity and alter substrate  
226 transformation pathways, causing the net CH<sub>4</sub> emission flux to stabilize or decline (Fairbairn et al. 2023,  
227 Zhang et al. 2024).

228           This study found that the temperature sensitivity ( $Q_{10}$ ) of both CO<sub>2</sub> and CH<sub>4</sub> emissions reached its



229 minimum value under optimal soil water content conditions. This key finding suggests that under  
230 non-limiting, suitable water conditions, microbial metabolic processes exhibit a relatively reduced  
231 dependence on temperature changes. Research indicates that this may imply that under such conditions,  
232 substrate availability replaces the activation energy required for reaction kinetics as the dominant  
233 rate-limiting factor controlling respiration rates (He et al. 2023). Simultaneously, changes in soil water  
234 content conditions further modulate the expression of temperature sensitivity by influencing the  
235 transport and transformation of dissolved organic carbon (Feng et al. 2020). However, a complete  
236 consensus has not been reached in the academic community regarding the effect of soil water content  
237 on  $Q_{10}$ . These discrepancies highlight the complexity of the soil water content-temperature response  
238 relationship, which may be modulated by a combination of factors such as ecosystem type, soil matrix  
239 conditions, and microbial community structure (Domeignoz - Horta et al. 2023).

240 In the specific context of saline-alkaline soils, the soil water content effect also exhibits significant  
241 interactions with salinity. For instance, regarding  $CO_2$  emissions, appropriate soil water content can to  
242 some extent alleviate the osmotic stress and ion-specific toxicity imposed by salinity on microorganisms.  
243 Consequently, the inhibitory effect of salinity is often weaker at medium soil water content levels (e.g.,  
244 60% WFPS) than at high soil water content levels (e.g., 90% WFPS) (Thapa et al. 2017, Zhang et al.  
245 2018).

#### 246 **4.2. Salinity as a key suppressor and modifier of temperature response**

247 Salinity is another core environmental factor regulating greenhouse gas emissions and their  
248 temperature responses in saline-alkaline ecosystems. This study, along with extensive literature,  
249 confirms that elevated salinity generally suppresses both  $CO_2$  and  $CH_4$  emission fluxes (Haj-Amor et al.  
250 2022, Yang et al. 2023). The underlying inhibitory mechanisms primarily include the following aspects:  
251 First, salinity directly affects microbial physiological activity and biomass by inducing osmotic stress  
252 and ion-specific toxicity (Lin et al. 2021). Second, it reduces the availability of labile carbon and nitrogen  
253 substrates and inhibits the activity of extracellular enzymes crucial for organic matter decomposition,  
254 such as  $\beta$ -glucosidase (Qu et al. 2022). Third, salinity profoundly alters the abundance and composition  
255 of microbial communities and functional genes. For instance, in saline-alkaline soils, the abundance of  
256 methanogenesis-related functional genes (e.g., *mcrA*) decreases with increasing salinity, while methane



257 oxidation-related genes (e.g., *pmoA*) may also decline. Overall, the microbial community balance shifts  
258 toward suppressing net CH<sub>4</sub> production (Yang et al. 2023). Low substrate availability is a significant  
259 factor limiting gas production in saline soils, although the addition of organic amendments can partially  
260 alleviate this limitation (Nguyen et al. 2020).

261 A key and more complex finding is that while salinity suppresses the absolute magnitude of gas  
262 emissions, it can significantly alter their temperature sensitivity ( $Q_{10}$ ). For CO<sub>2</sub> emissions, although  
263 cumulative emissions are lower in high-salinity soils, their  $Q_{10}$  values (reported in the range of 2.6 to  
264 5.2) increase significantly with rising salinity (Yu et al. 2020, Haj-Amor et al. 2022). This implies that  
265 under climate warming, saline-alkaline soils may release a proportionally greater amount of CO<sub>2</sub> per  
266 degree of temperature increase compared to non-saline soils, potentially amplifying the positive  
267 feedback to warming. This enhancement of  $Q_{10}$  may be related to salinity altering the thermodynamics  
268 of organic matter decomposition, for example, by shifting the microbial community toward reliance on  
269 more recalcitrant carbon pools or changing the dominant decomposition pathways (Zhang et al. 2023).  
270 For CH<sub>4</sub> emissions, the observed decrease in net flux with increasing salinity in this study indicates  
271 severe suppression of methanogenesis. The response pattern of its  $Q_{10}$  to salinity exhibits unique  
272 characteristics. This study found an increase in CH<sub>4</sub>  $Q_{10}$  with rising salinity, suggesting that the residual  
273 methanogenic microbial communities or processes in high-salinity environments may have stronger  
274 temperature dependence (Cai et al. 2025). This could result from a shift in community structure toward  
275 more stress-tolerant taxa whose metabolism is highly temperature-sensitive, or from a temperature-  
276 dependent alleviation of ionic stress. However, other evidence suggests that due to severe limitations in  
277 methanogen activity and substrate availability, the overall temperature sensitivity of CH<sub>4</sub> emissions in  
278 high-salinity soils may be lower (Zhou et al. 2018). Such discrepancies likely arise from differences in  
279 specific environmental conditions and experimental designs.

#### 280 4.3. Implications and future perspectives

281 This study provides novel empirical data on the  $Q_{10}$  of greenhouse gases in coastal saline-alkaline  
282 soils, addressing a research gap that has previously focused largely on forests and peatlands (Heffernan  
283 et al. 2024, Li et al. 2025). The results demonstrate that the temperature sensitivity of carbon cycling is  
284 not a fixed ecosystem property but is dynamically regulated by abiotic stressors such as soil water



285 content and salinity. A key management implication from this study is that optimal soil water content  
286 conditions can minimize the  $Q_{10}$  of carbon emissions. This suggests that through rational water  
287 management, it may be possible not only to regulate the immediate carbon emission flux from saline-  
288 alkaline lands but also to reduce the sensitivity of these emissions to future climate warming.

289 For predictive modeling, incorporating the nonlinear and interactive effects of soil water content  
290 and salinity is crucial for improving the accuracy of climate-carbon feedback projections in vulnerable  
291 coastal zones under scenarios of sea-level rise, altered precipitation patterns, and increased evaporation  
292 (Valiela et al. 2018, Richey et al. 2025). Future research needs to further elucidate the specific  
293 mechanisms by which salinity-moisture-temperature interactions affect microbial functions and  
294 community succession. Integrating these multi-factor coupled responses into regional and global carbon  
295 cycle models is essential to enhance the predictive capability for carbon dynamics in saline-alkaline  
296 ecosystems, thereby providing a solid scientific foundation for addressing climate change and achieving  
297 sustainable land management.

## 298 **5. Conclusions**

299 This study demonstrates that soil water content and salinity jointly regulate the temperature  
300 sensitivity ( $Q_{10}$ ) of  $CO_2$  and  $CH_4$  emissions in coastal saline-alkaline land. The unimodal response of  
301 gas fluxes to soil water content, with optimal emissions and minimized  $Q_{10}$  at 45% soil water content,  
302 highlights soil water content's critical role. Elevated salinity generally suppressed emissions but  
303 increased the  $Q_{10}$  of  $CH_4$ , revealing a stress-induced shift in microbial temperature dependence.  
304 Significant interactions between these factors were observed, underscoring that their combined effects,  
305 rather than individual impacts, dictate the net climate feedback. These findings validate our initial  
306 hypotheses and fill a key knowledge gap regarding carbon cycling in dynamic coastal ecosystems.  
307 Incorporating such non-linear interactions into carbon-climate models is essential for improving  
308 predictions of greenhouse gas emissions under global change in vulnerable saline-affected regions.

## 309 **Acknowledgments**

310 This study was supported by grants from the China Agriculture Research System (CARS-  
311 34-19), and the “Youth Innovation Team Plan” of Universities in Shandong Province  
312 (2022KJ166).



313 **References**

- 314 Alster, C. J., Z. D. Weller, et al., A meta-analysis of temperature sensitivity as a microbial trait. *Global Change*  
315 *Biology*; 2018. 24(9): 4211–4224
- 316 Cai, M., P. Zhang, et al., Salinity and nutrient availability dictate methane production and its temperature  
317 sensitivity in lakes. *Water Research*; 2025: 124836
- 318 Cao, X., S. Tang, et al., Effects of plant communities on the emission of soil greenhouse gases in riparian  
319 wetlands during spring thaw. *Ecohydrology*; 2023. 16(2): e2496
- 320 Capocci, M., J. Barba, et al., Experimental influence of storm-surge salinity on soil greenhouse gas emissions  
321 from a tidal salt marsh. *Science of the Total Environment*; 2019. 686: 1164–1172
- 322 Domeignoz-Horta, L. A., G. Pold, et al., Substrate availability and not thermal acclimation controls microbial  
323 temperature sensitivity response to long-term warming. *Global Change Biology*; 2023. 29(6): 1574–1590
- 324 Fairbairn, L., F. Rezanezhad, et al., Relationship between soil CO<sub>2</sub> fluxes and soil moisture: Anaerobic sources  
325 explain fluxes at high water content. *Geoderma*; 2023. 434: 116493
- 326 Feng, X., M. J. Deventer, et al., Climate sensitivity of peatland methane emissions mediated by seasonal  
327 hydrologic dynamics. *Geophysical Research Letters*; 2020. 47(17): e2020GL088875
- 328 Feng, Z., L. Wang, et al., Responses of soil greenhouse gas emissions to land use conversion and reversion—A  
329 global meta-analysis. *Global Change Biology*; 2022. 28(22): 6665–6678
- 330 Gao, B., T. Huang, et al., Chinese cropping systems are a net source of greenhouse gases despite soil carbon  
331 sequestration. *Global change biology*; 2018. 24(12): 5590–5606
- 332 Gao, D., B. Peng, et al., Different winter soil respiration between two mid-temperate plantation forests. *Forest*  
333 *Ecology and Management*; 2018. 409: 390–398
- 334 Gondwe, M., C. Helfter, et al., Methane flux measurements along a floodplain soil moisture gradient in the  
335 Okavango Delta, Botswana. *Philosophical Transactions of the Royal Society A*; 2021. 379(2210): 20200448
- 336 Haj-Amor, Z., T. Araya, et al., Soil salinity and its associated effects on soil microorganisms, greenhouse gas  
337 emissions, crop yield, biodiversity and desertification: A review. *Science of The Total Environment*; 2022.  
338 843: 156946
- 339 Hansen, R., Ü. Mander, et al., Greenhouse gas fluxes in an open air humidity manipulation experiment.  
340 *Landscape Ecology*; 2013. 28(4): 637–649
- 341 He, Y., X. Zhou, et al., Apparent thermal acclimation of soil heterotrophic respiration mainly mediated by  
342 substrate availability. *Global Change Biology*; 2023. 29(4): 1178–1187
- 343 Heffernan, L., C. Estop-Aragónés, et al., Changing climatic controls on the greenhouse gas balance of  
344 thermokarst bogs during succession after permafrost thaw. *Global Change Biology*; 2024. 30(7): e17388
- 345 Ho, L., M. Barthel, et al., Regulating greenhouse gas dynamics in tidal wetlands: Impacts of salinity gradients  
346 and water pollution. *Journal of Environmental Management*; 2024. 364: 121427
- 347 Huang, C.-M., C.-S. Yuan, et al., Temporal variations of greenhouse gas emissions and carbon sequestration and  
348 stock from a tidal constructed mangrove wetland. *Marine Pollution Bulletin*; 2019. 149: 110568
- 349 Huang, K., J. Kuai, et al., Effects of understory intercropping with salt-tolerant legumes on soil organic carbon  
350 pool in coastal saline-alkali land. *Journal of Environmental Management*; 2024. 370: 122677
- 351 Johnston, A. S. and R. M. Sibly, The influence of soil communities on the temperature sensitivity of soil  
352 respiration. *Nature ecology & evolution*; 2018. 2(10): 1597–1602
- 353 Lang, R., S. Blagodatsky, et al., Seasonal differences in soil respiration and methane uptake in rubber plantation  
354 and rainforest. *Agriculture, Ecosystems & Environment*; 2017. 240: 314–328



- 355 Li, H., S. Yang, et al., Temperature sensitivity of SOM decomposition is linked with a K-selected microbial  
356 community. *Global Change Biology*; 2021. 27(12): 2763–2779
- 357 Li, J., L. Ma, et al., Greenhouse gas emissions from different vegetation types in the permafrost region of the  
358 Daxing'an Mountains under drying-rewetting conditions. *Journal of Environmental Management*; 2025. 380:  
359 125178
- 360 Li, J., M. Nie, et al., Biogeographic variation in temperature sensitivity of decomposition in forest soils. *Global*  
361 *Change Biology*; 2020. 26(3): 1873–1885
- 362 Lin, L., S. Pratt, et al., Salinity effect on freshwater Anammox bacteria: Ionic stress and ion composition. *Water*  
363 *Research*; 2021. 188: 116432
- 364 Liu, Y., X. Lan, et al., Multifaceted ability of organic fertilizers to improve crop productivity and abiotic stress  
365 tolerance: Review and perspectives. *Agronomy*; 2024. 14(6): 1141
- 366 Lloyd, J. and J. Taylor, On the temperature dependence of soil respiration. *Functional ecology*; 1994: 315–323
- 367 Ma, C., P. Song, et al., Optimizing Phosphorus Fertilization for Enhanced Yield and Nutrient Efficiency of Wheat  
368 (*Triticum aestivum* L.) on Saline–Alkali Soils in the Yellow River Delta, China. *Land*; 2025. 14(6): 1241
- 369 Ma, S., Y. Li, et al., Determinants of rhizospheric organic carbon fractions and accumulation in four different  
370 vegetations of coastal saline-alkali soils. *Catena*; 2024. 246: 108454
- 371 Ma, Z., Y. Zhu, et al., Multi-objective optimization of saline water irrigation in arid oasis regions: Integrating  
372 water-saving, salinity control, yield enhancement, and CO<sub>2</sub> emission reduction for sustainable cotton  
373 production. *Science of the Total Environment*; 2024. 912: 169672
- 374 Nguyen, B. T., N. N. Trinh, et al., Methane emissions and associated microbial activities from paddy salt-affected  
375 soil as influenced by biochar and cow manure addition. *Applied Soil Ecology*; 2020. 152: 103531
- 376 Niu, Y., Y. Li, et al., Microbial transformation mechanisms of particulate organic carbon to mineral-associated  
377 organic carbon at the chemical molecular level: highlighting the effects of ambient temperature and soil  
378 moisture. *Soil Biology and Biochemistry*; 2024. 195: 109454
- 379 Pathak, H. and D. Rao, Carbon and nitrogen mineralization from added organic matter in saline and alkali soils.  
380 *Soil biology and biochemistry*; 1998. 30(6): 695–702
- 381 Peng, J., S. Xie, et al., Global Evidence of the Unimodal Response of Ecosystem Respiration to Soil Moisture.  
382 *Advanced Science*; 2025: e09753
- 383 Qu, Y., J. Tang, et al., Rhizosphere enzyme activities and microorganisms drive the transformation of organic  
384 and inorganic carbon in saline–alkali soil region. *Scientific Reports*; 2022. 12(1): 1314
- 385 Richey, A., S. F. Oberbauer, et al., Sea-level rise and freshwater management are reshaping coastal landscapes.  
386 *Journal of Environmental Management*; 2025. 387: 125842
- 387 Saari, A., A. Smolander, et al., Methane consumption in a frequently nitrogen-fertilized and limed spruce forest  
388 soil after clear-cutting. *Soil Use and Management*; 2004. 20(1): 65–73
- 389 Schaufler, G., B. Kitzler, et al., Greenhouse gas emissions from European soils under different land use: effects  
390 of soil moisture and temperature. *European Journal of Soil Science*; 2010. 61(5): 683–696
- 391 Suh, S., E. Lee, et al., Temperature and moisture sensitivities of CO<sub>2</sub> efflux from lowland and alpine meadow  
392 soils. *Journal of Plant Ecology*; 2009. 2(4): 225–231
- 393 SUN, B.-Y., G.-X. HAN, et al., Effects of elevated temperature on soil respiration in a coastal wetland during  
394 the non-growing season in the Yellow River Delta, China. *Chinese Journal of Plant Ecology*; 2016. 40(11):  
395 1111–1123



- 396 Tang, J., S. Liang, et al., Emission laws and influence factors of greenhouse gases in saline-alkali paddy fields.  
397 Sustainability; 2016. 8(2): 163
- 398 Thapa, R., A. Chatterjee, et al., Carbon dioxide and nitrous oxide emissions from naturally occurring sulfate-  
399 based saline soils at different moisture contents. Pedosphere; 2017. 27(5): 868–876
- 400 Valiela, I., J. Lloret, et al., Transient coastal landscapes: Rising sea level threatens salt marshes. Science of the  
401 Total Environment; 2018. 640: 1148–1156
- 402 Wang, B., T. Zha, et al., Soil moisture modifies the response of soil respiration to temperature in a desert shrub  
403 ecosystem. Biogeosciences; 2013. 10: 9213–9242
- 404 Wang, P., J. Wang, et al., Soil Moisture Threshold of Methane Uptake in Alpine Grassland Ecosystems. Global  
405 Change Biology; 2025. 31(2): e70062
- 406 Wang, Q., S. Liu, et al., Carbon quality and soil microbial property control the latitudinal pattern in temperature  
407 sensitivity of soil microbial respiration across Chinese forest ecosystems. Global change biology; 2018.  
408 24(7): 2841–2849
- 409 Wang, X., S. Piao, et al., A two-fold increase of carbon cycle sensitivity to tropical temperature variations.  
410 Nature; 2014. 506(7487): 212–215
- 411 Wang, X., J. Wang, et al., Seasonality of soil respiration under gypsum and straw amendments in an arid saline-  
412 alkali soil. Journal of Environmental Management; 2021. 277: 111494
- 413 Wong, V. N., R. Greene, et al., Soil carbon dynamics in saline and sodic soils: a review. Soil use and management;  
414 2010. 26(1): 2–11
- 415 Yang, C., Y. Chen, et al., Extreme soil salinity reduces N and P metabolism and related microbial network  
416 complexity and community immigration rate. Environmental Research; 2025. 264: 120361
- 417 Yang, C., Y. Chen, et al., Mechanism of microbial regulation on methane metabolism in saline-alkali soils based  
418 on metagenomics analysis. Journal of Environmental Management; 2023. 345: 118771
- 419 Yang, Y., T. Li, et al., Global effects on soil respiration and its temperature sensitivity depend on nitrogen addition  
420 rate. Soil Biology and Biochemistry; 2022. 174: 108814
- 421 Yin, J., J. Li, et al., Soil moisture and abundance of microbial groups are key determinants of greenhouse gas  
422 fluxes in a semi-arid wetland ecosystem. Journal of Environmental Management; 2025. 390: 126296
- 423 Yu, Y., X. Li, et al., Soil salinity changes the temperature sensitivity of soil carbon dioxide and nitrous oxide  
424 emissions. Catena; 2020. 195: 104912
- 425 Zeeshan, M., Z. Wenjun, et al., Soil heterotrophic respiration in response to rising temperature and moisture  
426 along an altitudinal gradient in a subtropical forest ecosystem, Southwest China. Science of The Total  
427 Environment; 2022. 816: 151643
- 428 Zhan, P.-F. and C. Tong, Methane emissions partially offset carbon sink function in global wetlands: An analysis  
429 based on global data. Ying Yong Sheng tai xue bao= The Journal of Applied Ecology; 2023. 34(11): 2958–  
430 2968
- 431 Zhang, G., J. Bai, et al., Soil microbial communities regulate the threshold effect of salinity stress on SOM  
432 decomposition in coastal salt marshes. Fundamental research; 2023. 3(6): 868–879
- 433 Zhang, L., W. Lin, et al., Soil warming-induced reduction in water content enhanced methane uptake at different  
434 soil depths in a subtropical forest. Science of The Total Environment; 2024. 927: 171994
- 435 Zhang, L., L. Song, et al., Co-effects of salinity and moisture on CO<sub>2</sub> and N<sub>2</sub>O emissions of laboratory-incubated  
436 salt-affected soils from different vegetation types. Geoderma; 2018. 332: 109–120



437 Zhou, M., X. Wang, et al., A three-year experiment of annual methane and nitrous oxide emissions from the  
438 subtropical permanently flooded rice paddy fields of China: Emission factor, temperature sensitivity and  
439 fertilizer nitrogen effect. *Agricultural and Forest Meteorology*; 2018. 250: 299–307  
440  
441



442 **Table 1 Basic properties of the incubation soil for the experiment**

Soil properties	S1	S2	S3	S4	S5
EC (dS/m)	1.9 (0.1)	10.8(1)	58.8 (6.2)	66.3 (7.3)	96.0 (12)
Salt (g/kg)	1.19 (0.38)	1.49 (0.26)	5.15 (0.66)	7.56 (0.97)	8.10 (1.32)
pH	8.29 (0.05)	8.29 (0.09)	7.92(0.04)	7.86 (0.07)	8.03 (0.05)
TC (g/kg)	14.71 (0.10)	12.99 (0.17)	15.88 (0.18)	13.65 (0.26)	12.67 (0.09)
TN (g/kg)	0.34 (0.01)	0.29 (0.01)	0.33 (0.01)	0.31 (0.01)	0.27 (0.01)
C/N ratio	43.48 (1.00)	45.15 (1.11)	48.06 (0.57)	44.63 (0.96)	47.26 (1.00)

443

444 **Table 2 Effect of soil water content on CO<sub>2</sub> and CH<sub>4</sub> temperature sensitivity**

Water content (%)	CO <sub>2</sub>		CH <sub>4</sub>		445
	b	Q <sub>10</sub>	b	Q <sub>10</sub>	
5	0.0573±0.0045	1.7735±0.0816	0.0216±0.0062	1.2411±0.0794	
15	0.0625±0.0055	1.8681±0.1056	0.0251±0.0063	1.2853±0.0836	
30	0.0538±0.0061	1.7125±0.1077	0.0201±0.0069	1.2230±0.0873	
45	0.0393±0.0042	1.4814±0.0635	0.0118±0.0054	1.1252±0.0624	
60	0.0593±0.0039	1.8093±0.0719	0.0151±0.0041	1.1630±0.0487	

446 **Table 3 Effect of soil salinity (EC) on CO<sub>2</sub> and CH<sub>4</sub> temperature sensitivity**

EC (ds/m)	CO <sub>2</sub>		CH <sub>4</sub>		447
	b	Q <sub>10</sub>	b	Q <sub>10</sub>	
1.9	0.0489±0.0035	1.6306±0.0581	0.0156±0.0031	1.1688±0.0368	448
10.8	0.0556±0.0051	1.7458±0.0912	0.0113±0.0058	1.1196±0.0669	
58.8	0.0412±0.0064	1.5098±0.0998	0.0183±0.0064	1.2008±0.0794	
66.3	0.0362±0.0042	1.4361±0.0616	0.0255±0.0055	1.2904±0.0730	
96.0	0.0467±0.0055	1.5951±0.0902	0.0326±0.0057	1.3854±0.0813	

449

**Figure captions**



450 **Figure 1.** CO<sub>2</sub> emission flux across temperature gradients under different soil water content treatments.  
451 Significant differences ( $P < 0.05$ ) among water content treatments at the same temperature are indicated  
452 by lowercase letters; differences among temperature treatments at the same water content are indicated  
453 by uppercase letters.

454 **Figure 2.** CH<sub>4</sub> emission flux across temperature gradients under different soil water content treatments.  
455 Significant differences ( $P < 0.05$ ) among water content treatments at the same temperature are indicated  
456 by lowercase letters; differences among temperature treatments at the same water content are indicated  
457 by uppercase letters.

458 **Figure 3.** Exponential relationships between soil CO<sub>2</sub> emission flux and soil water content at six  
459 incubation temperatures (5, 10, 15, 20, 25, and 30°C; panels a–f). All relationships are significant ( $P <$   
460 0.05), with the coefficient of determination ( $R^2$ ) shown in each panel.

461 **Figure 4.** Exponential relationships between soil CH<sub>4</sub> emission flux and soil water content at six  
462 incubation temperatures (5, 10, 15, 20, 25, and 30°C; panels a–f). All relationships are significant ( $P <$   
463 0.05), with the coefficient of determination ( $R^2$ ) shown in each panel.

464 **Figure 5.** CO<sub>2</sub> emission flux across temperature gradients under different soil salinity (EC) treatments.  
465 Significant differences ( $P < 0.05$ ) among salinity treatments at the same temperature are indicated by  
466 lowercase letters; differences among temperature treatments at the same salinity level are indicated by  
467 uppercase letters.

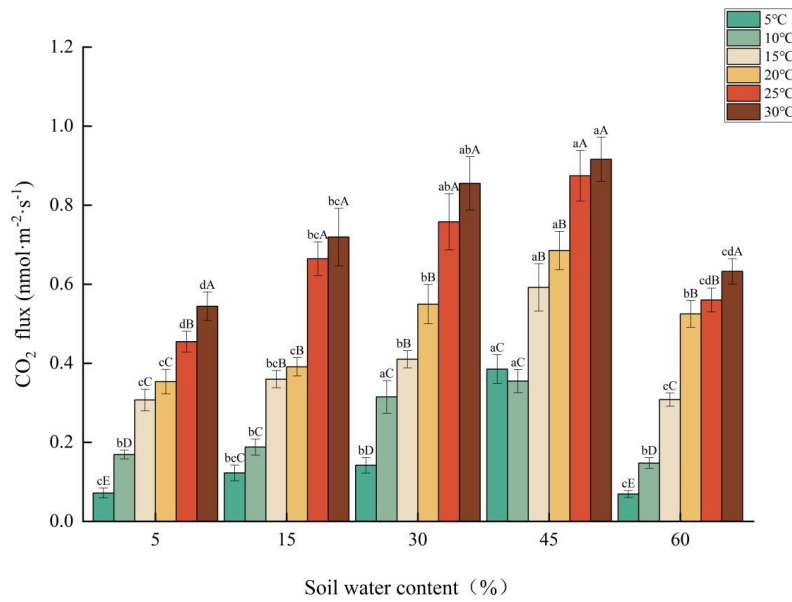
468 **Figure 6.** CH<sub>4</sub> emission flux across temperature gradients under different soil salinity (electrical  
469 conductivity, EC) treatments. Significant differences ( $P < 0.05$ ) among salinity treatments at the same  
470 temperature are indicated by lowercase letters; differences among temperature treatments at the same  
471 salinity level are indicated by uppercase letters.

472 **Figure 7.** Exponential relationships between soil CO<sub>2</sub> emission flux and soil salinity (EC) at six  
473 incubation temperatures (5, 10, 15, 20, 25, and 30°C; panels a–f). All relationships are significant ( $P <$   
474 0.05), with the coefficient of determination ( $R^2$ ) shown in each panel.

475 **Figure 8.** Exponential relationships between soil CH<sub>4</sub> emission flux and soil salinity (EC) at six  
476 incubation temperatures (5, 10, 15, 20, 25, and 30°C; panels a–f). All relationships are significant ( $P <$   
477 0.05), with the coefficient of determination ( $R^2$ ) shown in each panel.



478 **Figure 1**

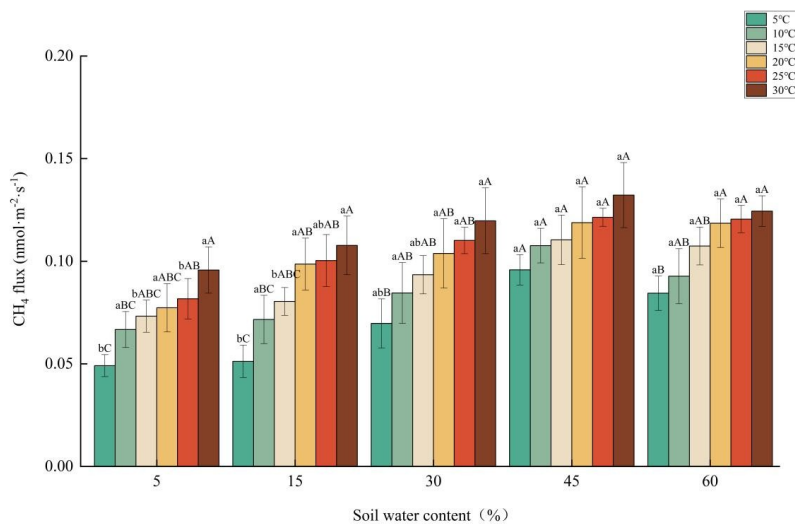


479

480



481 **Figure 2**

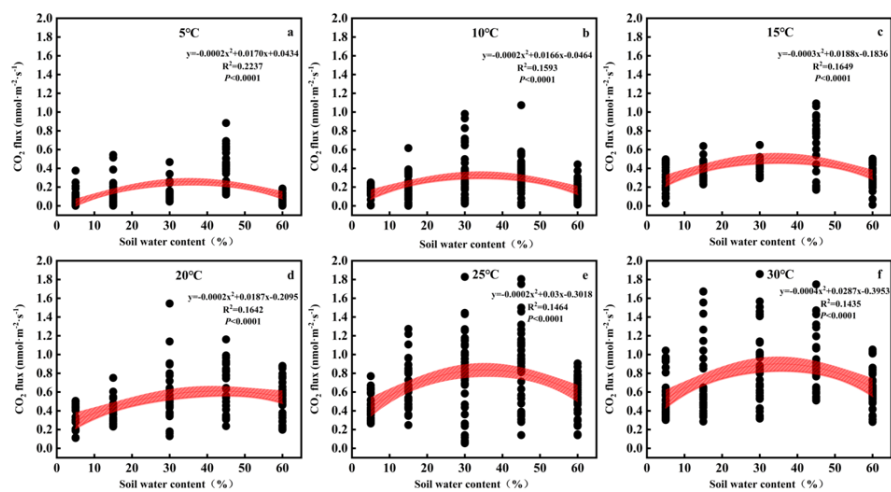


482

483



484 **Figure 3**

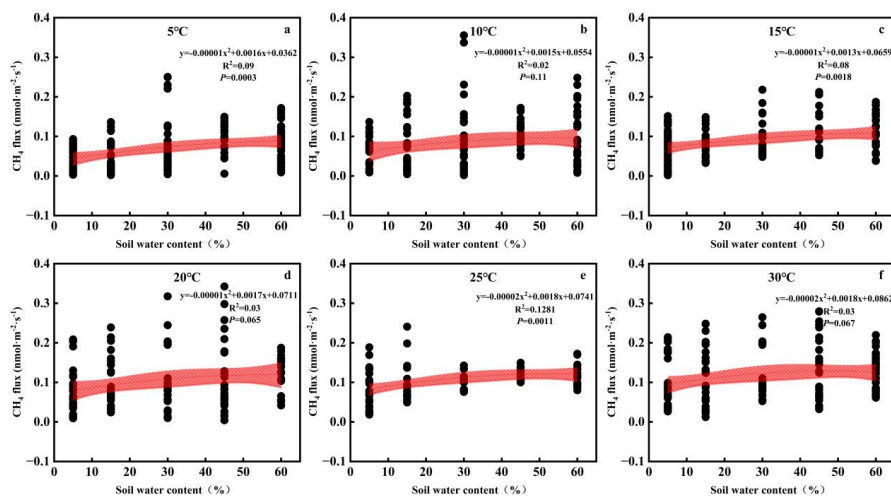


485

486



487 **Figure 4**

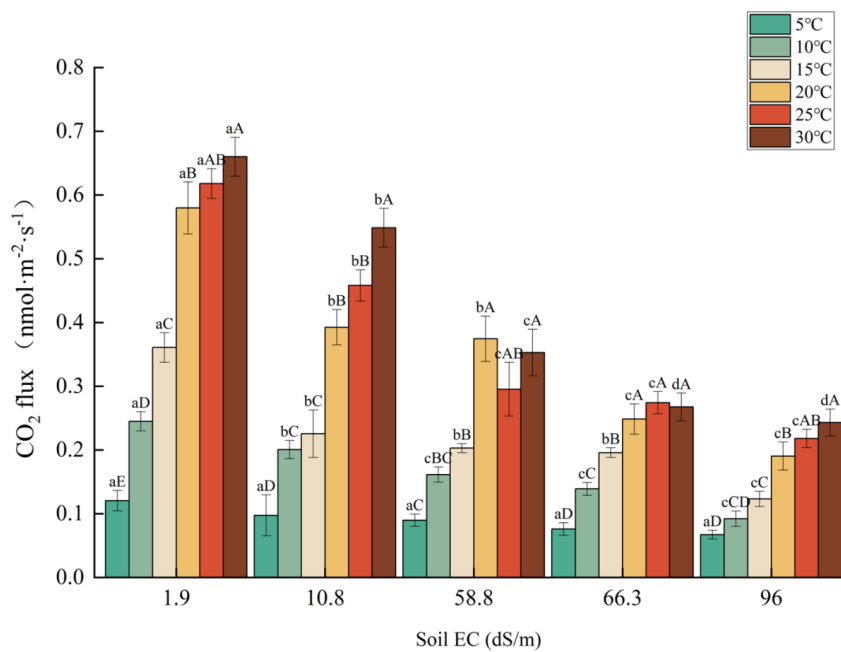


488

489



490 **Figure 5**

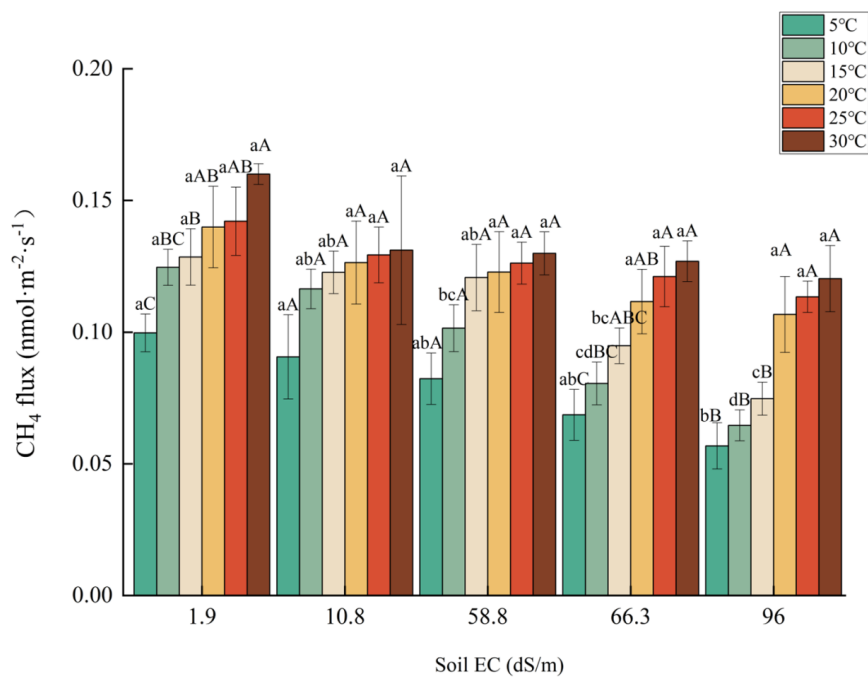


491

492



493 **Figure 6**

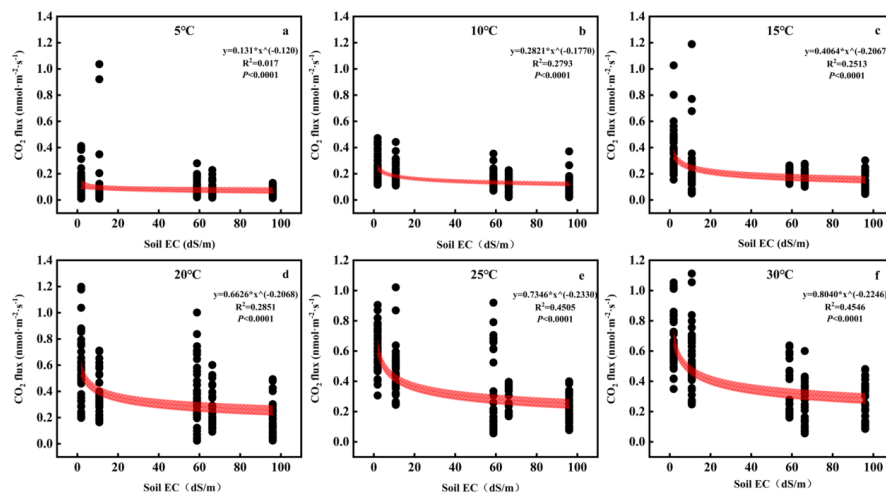


494

495



496 **Figure 7**

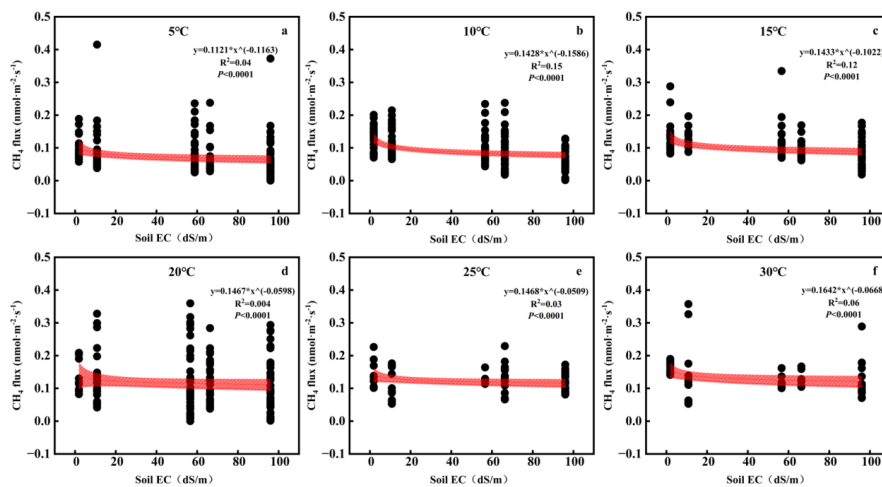


497

498



499 **Figure 8**



500